TEM Calibration Methods for Critical Dimension Standards

Ndubuisi G. Orji[a], Ronald G. Dixson[a], Domingo I. Garcia-Gutierrez[b], Benjamin D. Bunday[c], Michael Bishop[c], Michael W. Cresswell[a], Richard A. Allen[a], John A. Allgair[c]
[a]National Institute of Standards and Technology, 100 Bureau Drive, Gaithersburg, MD 20899-8212[†]
[b]Advanced Technology Development Facility (ATDF), Austin, TX 78741
[c]International SEMATECH Manufacturing Initiative (ISMI), Austin, TX, 78741[‡]

ABSTRACT

One of the key challenges in critical dimension (CD) metrology is finding suitable calibration standards. Over the last few years there has been some interest in using features measured with the transmission electron microscope (TEM) as primary standards for linewidth measurements. This is because some modes of TEM can produce lattice-resolved images having scale traceability to the SI (*Système International d'Unites* or International System of Units) definition of length through an atomic lattice constant. As interest in using calibration samples that are closer to the length scales being measured increases, so will the use of these TEM techniques.

An area where lattice-traceable images produced by TEM has been used as a primary standard is in critical dimension atomic force microscope (CD-AFM) tip width calibration. Two modes of TEM that produce crystal lattice-traceable images are high resolution transmission electron microscope (HR-TEM) and high angle annular dark field scanning transmission electron microscope (HAADF-STEM). HR-TEM produces lattice-traceable images by interference patterns of the diffracted and transmitted beams rather than the actual atomic columns, while HAADF-STEM produces direct images of the crystal lattice. The difference in how both of these techniques work could cause subtle variations in the way feature edges are defined.

In this paper, we present results from width samples measured using HR-TEM and HAADF-STEM. Next we compare the results with measurements taken from the same location by two different CD-AFMs.

Both of the CD-AFM instruments used for this work have been calibrated using a single crystal critical dimension reference material (SCCDRM). These standards, developed by the National Institute of Standards and Technology (NIST) and SEMATECH, used HR-TEM for traceable tip-width calibration. Consequently, the present work and the previous SCCDRM work provide a mutual cross-check on the traceability of the width calibration. Excellent agreement was observed.

Keywords: Linewidth, HR-TEM, HAADF-STEM, CD-AFM

1. INTRODUCTION

As the size of features in semiconductor manufacturing continues to decrease, measurement requirements are becoming more challenging. The *International Technology Roadmap for Semiconductors* (ITRS) [1] specifies that the physical gate length for 2013 should be 13 nm and inline non-destructive microscopy resolution for the same year should be 0.12 nm. Such requirements place a great deal of demand on the instruments that measure critical dimensions (CDs). One of the key enablers to achieving current and future metrology requirements is the calibration and characterization of the instruments used for both process development and control.

Over the last few years, samples measured with the transmission electron microscope (TEM) have been used as standards for linewidth measurements [2-6]. At high magnification in some TEM modes, the lattice periodicity can be

Metrology, Inspection, and Process Control for Microlithography XXI, edited by Chas N. Archie
Proc. of SPIE Vol. 6518, 651810, (2007) · 0277-786X/07/$18 · doi: 10.1117/12.713368

resolved. Consequently, the image scale can be traceable to the SI (*Système International d'Unites* or International System of Units) definition of length through an atomic lattice constant. One area where these types of features have been used is in calibrating the tip width of critical dimension atomic force microscopes (CD-AFMs). In our previous work [2], we used features imaged with high resolution TEM (HR-TEM) to characterize artifacts for CD-AFM tip width calibration. The mode of TEM mostly used for this type of calibration is HR-TEM, which produces lattice-traceable images by interference patterns of the diffracted and transmitted beams. Given that the lattice positions are not directly imaged, there are concerns that the interference patterns may not be as accurate as the calibration application may require. Another mode of TEM, known as high angle annular dark field scanning transmission electron microscope (HAADF-STEM), produces images that represent the locations of the actual atomic column. The difference in how both of these techniques work could cause subtle variations in how feature edges are defined.

In this paper, we present preliminary results of our evaluation of a calibration sample measured with both the HAADF-STEM and HR-TEM and compare the results. The samples are first measured with two different CD-AFMs that are implemented as reference measurement systems (RMS), and then cross-sectioned and characterized with the two TEM modes. The results from this work will serve two purposes. One goal is to compare two different modes of the TEM with respect to the *SI* lattice constant to see how the results compare with practical calibration measurements. The second goal is to present a separate validation of our previous work using a different TEM imaging mode.

The paper is organized as follows. Section 2 introduces the instruments used in this study, TEM and CD-AFM. Section 3 describes the sample, measurement location and methods, and supporting comparison measurements. The TEM measurements and analysis are described in section 4, while section 5 gives some of the uncertainties associated with the study. The paper concludes with a summary in section 6.

2. INSTRUMENTATION

HR-TEM images are formed by the interference of the diffracted and transmitted electron beams. The images produced are from a coherent scattering of the electrons. They are not the actual atomic locations or columns [7]. A simplified schematic of a HR-TEM is shown in figure 1(a).

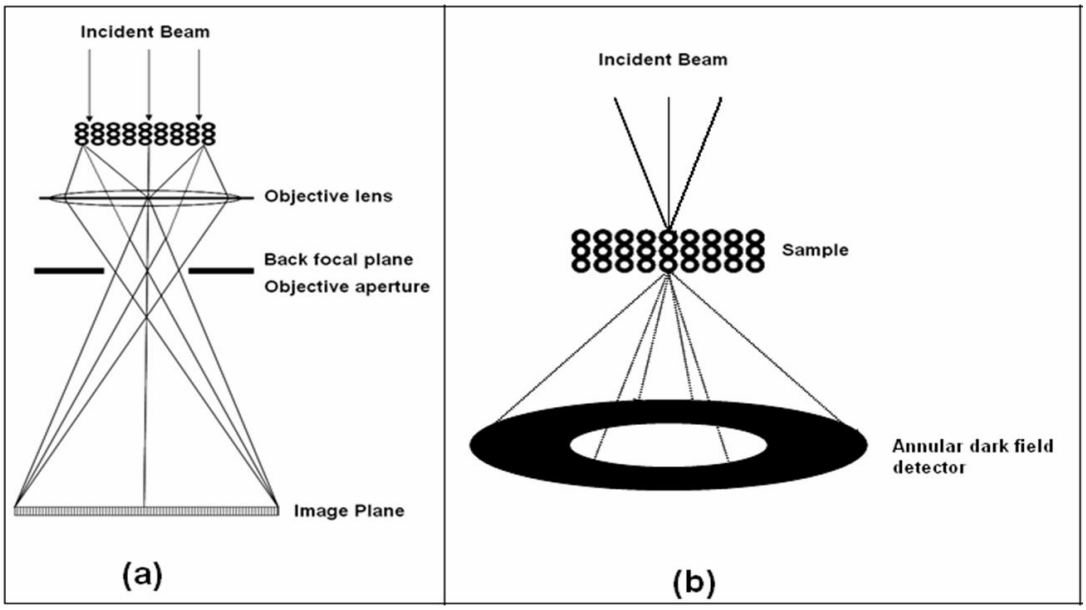

Figure 1: Schematic diagram of (a) HR-TEM imaging mode, (b) HAADF-STEM imaging mode.

In HAADF-STEM imaging, a focused electron probe is scanned across a thin sample [3]. The resulting scattered electrons, which comes from a single atom or atomic column, are detected by an annular ring detector where the

observed intensity is proportional to the Rutherford cross section (~Z^2) of the material [7,8]. A simplified schematic diagram of an HAADF-STEM is shown in figure 1(b). Note that the image for an HAADF-STEM is acquired point-by-point due to the interaction of the converged electron probe with the atomic columns from the sample, while the HR-TEM is acquired at the same time due to the parallel illumination on the sample. A key difference between the two techniques is that the HR-TEM image is coherent while the HAADF-STEM is not, because the image can be thought as the convolution between the electron probe with the atomic columns on the sample, this means that every atomic column will be an independent source of signal for the detector. This could lead to a slight difference in the way the beam interacts with the sample edge, which could result in different measured values. A detailed description of the differences between the two modes, best practices and approaches for reproducible measurements are given in Diebold et al. [9].

The CD-AFM is a two-dimensional AFM with the ability to sense in two directions. It uses a flared tip and specialized algorithms to access the sidewall of features and is well suited for making linewidth measurements. Images produced by the AFM usually contain the effect of the tip. Because of the sidewall scanning ability of the CD-AFM, this effect of the tip is easier to remove because it shows up as an additive offset to the apparent width. The tip width, which is known *a priori*, is used to account for this offset. Figure 2 shows a schematic image of a CD-AFM tip scanning over a feature. Both CD-AFMs used in this study are implemented as reference measurement systems [10, 11].

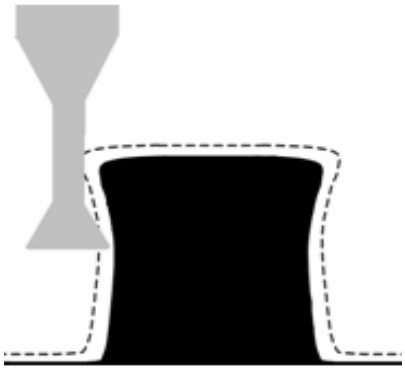

Figure 2: A schematic image of a CD-AFM tip scanning an undercut feature.

3. SAMPLE AND MEASUREMENTS

The type of sample used in this study is a single crystal critical dimension reference material (SCCDRM) [2]. The features on the SCCDRM samples are preferentially etched into a (110) silicon-on-insulator substrate, producing near vertical sidewalls. Since a key requirement for our experiment is that the features should be crystalline – providing the ability to use the lattice spacing as a "ruler" for the measurements – the SCCDRM is ideally suited for this work. The particular specimen used for this work was from the ongoing SCCDRM "next generation" thrust that is being reported elsewhere [12].

A schematic diagram of the SCCDRM layout is given in figure 3. The calibrations and uncertainty values for the SCCDRM sample are valid only along the marker center line; hence all the measurements were taken along the axis labeled reference line. This ensures that the same location is imaged by the CD-AFM and TEM. Additional information that verifies the measured location is in section 5. The second feature with a nominal size of 18 nm was used for the study. Note that the field of view accessible for HAADF-STEM mode is much smaller than that of HR-TEM, thereby restricting the sizes that could be imaged with both TEM modes. The samples were cross-sectioned for TEM (Figure 4) by focused ion beam (FIB) milling, using 30 kV Ga+ ions and a final beam current of ≈50 pA. The samples were characterized in an FEI TECNAI F30 ST™[§] analytical TEM operating at 300 keV.

[§] Certain commercial equipment is identified in this paper to adequately describe the experimental procedure. Such identification does not imply recommendation or endorsement by the National Institute of Standards and Technology or SEMATECH, nor does it imply that the equipment identified is necessarily the best available for the purpose.

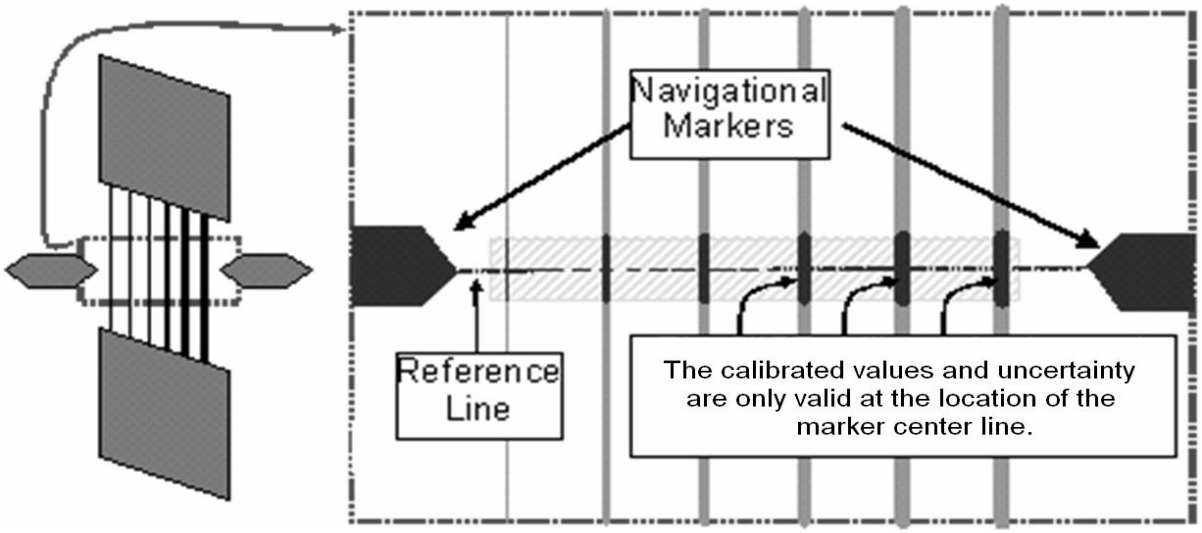

Figure 3: A schematic diagram of the SCCDRM sample. The sample is calibrated at the centerline location. The navigational markers aid in relocating the calibrated site.

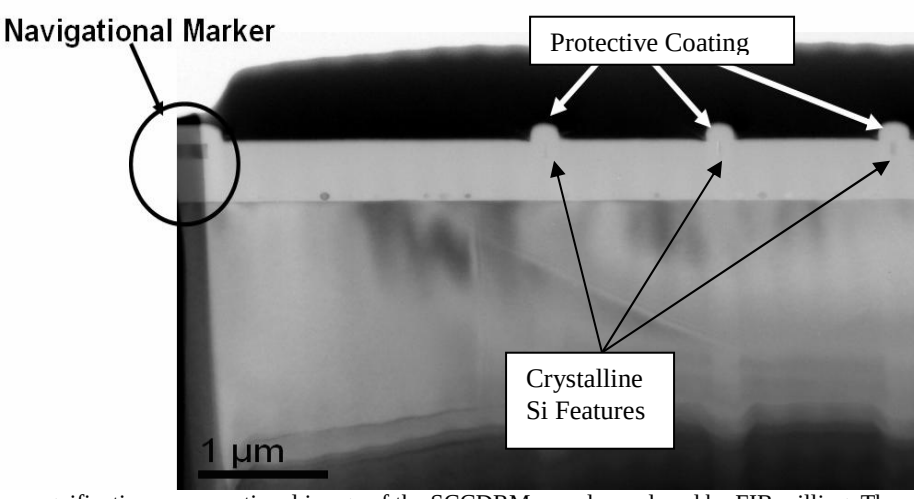

Figure 4: A low magnification cross-sectional image of the SCCDRM sample produced by FIB milling. The navigational marker shown on the left indicates that the sample was cross-sectioned at the right location.

In addition to the CD-AFM measurement of the cross-sectioned sample, we took additional data to compare the closeness of the results obtained using the two CD-AFMs. Figure 5 shows results of CD-AFM measurements on different targets that were taken at different times over a period of approximately one year using both instruments. Some of these samples were originally intended for preliminary TEM experiments at lower magnification. The slope of the regression line between the instruments is statistically consistent with unity. The average width offset between the two tools is about 0.25 nm – which is expected since both tools derive their tip width calibration from the SCCDRM 2004 release. The residual values that are larger than 1 nm are from features with sloped sidewalls, which usually have larger uncertainties due to higher order tip effects [13]. With respect to the present work, these comparisons provide important validation that nothing has changed in the tip width calibration of the two CD-AFM instruments we are using.

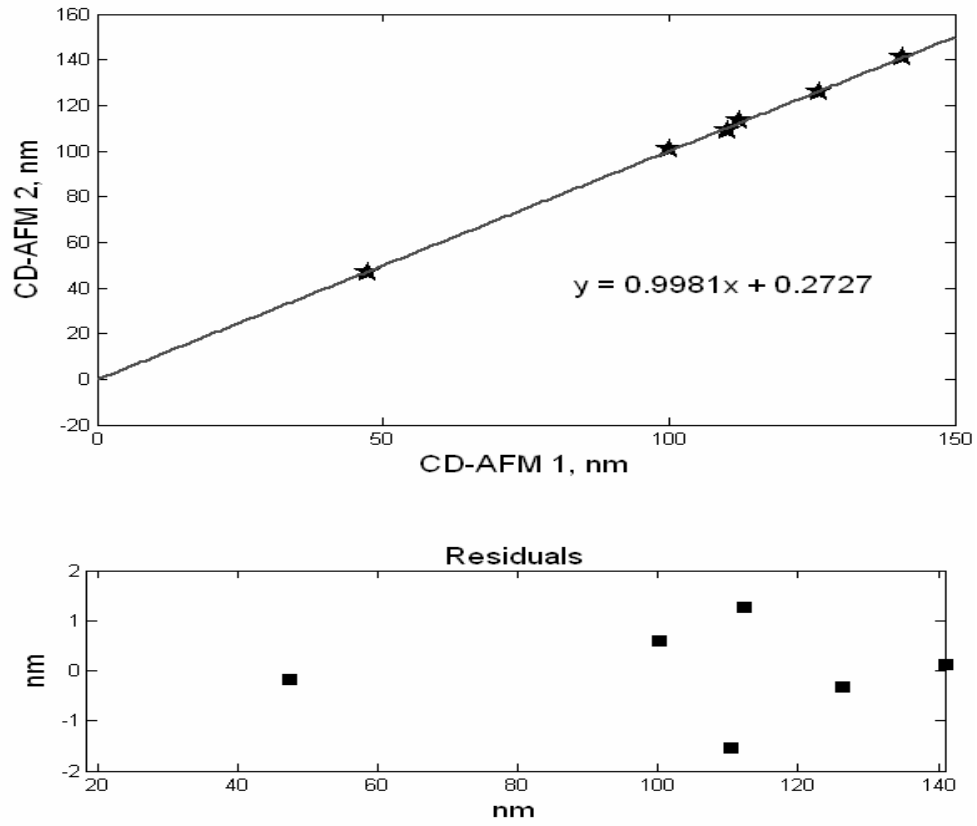

Figure 5: Comparison of measurements by two RMS CD-AFMs and the residuals. The slope of the regression line is statistically consistent with unity, and the average offset is approximately 0.25 nm .The samples with residuals of 1 nm or more have sloped sidewalls, which could introduce additional errors to the measurement due to higher-order tip effects.

4. TEM MEASUREMENTS AND ANALYSIS

HR-TEM images and HAADF-STEM images were taken from the same feature after cross-sectioning. The relatively small field of view (< 25 nm) required by the HAADF-STEM to see the atomic lattice prevented the use of larger samples. The sample was aligned for the z = [112] of the substrate silicon. The HAADF-STEM image was taken first followed by the HR-TEM. Figure 6 shows a HR-TEM image of the middle of the sample. Note that the field of view of the instrument did not allow the whole structure to be measured at high resolution. Figure 7 shows the corresponding HAADF-STEM image of the same feature.

The spacing in un-doped Si (111) is 0.313 560 137 nm with a standard uncertainty of ± 0.000 000 009 nm, as determined from X-ray diffraction [14]. The TEM images shown here are imaged as lines rather than individual atoms. This is due to the fact that in the [112] zone axis the two most important reflections contributing to the formation of the image are the {111} and the {220} crystallographic planes from the silicon FCC structure. Although in the image it looks like only the lines from the {111} planes can be observed, the smaller d-spacing from the {220} planes (0.1920148 nm), perpendicular to the {111} planes, can also be resolved at higher magnifications.

A close examination of the edges of the feature in the HR-TEM image shows five lines that cannot be specifically be assigned to part of the edge. These lines are highlighted in figure 8. Figure 7 shows an image of the same feature

obtained using HAADF-STEM. The left edge of the HAADF-STEM image shows two lines that cannot be assigned as part of the edge. These are highlighted in figure 9. It is also worth noting that the HAADF-STEM image shows a roll-off at the edges. This could be due to an aberration in the optics, although HR-TEM images are more sensitive to the aberrations in the optics of the microscopes than HAADF-STEM images. Figure 10 shows the results from the HR-TEM, HAADF-STEM and the two CD-AFMs. For the TEM results, the uncertainties shown include only the uncertainty in edge determination. The uncertainties for the CD-AFM results include all components except for an LWR/navigation term for direct comparison with the TEM values. (Note that the CD-AFM results derive their tip width calibration uncertainty independently from the series of HRTEM samples used in the SCCDRM project.)

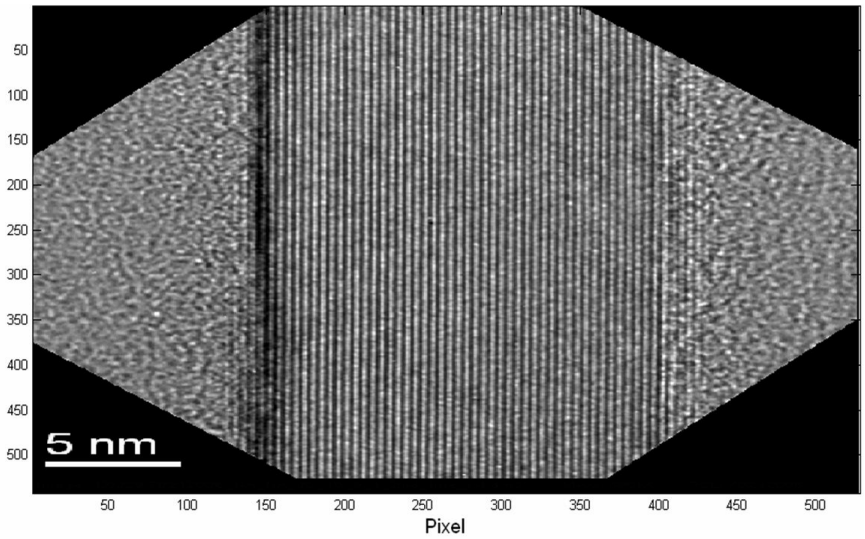

Figure 6: HR-TEM image of a SCCDRM feature.

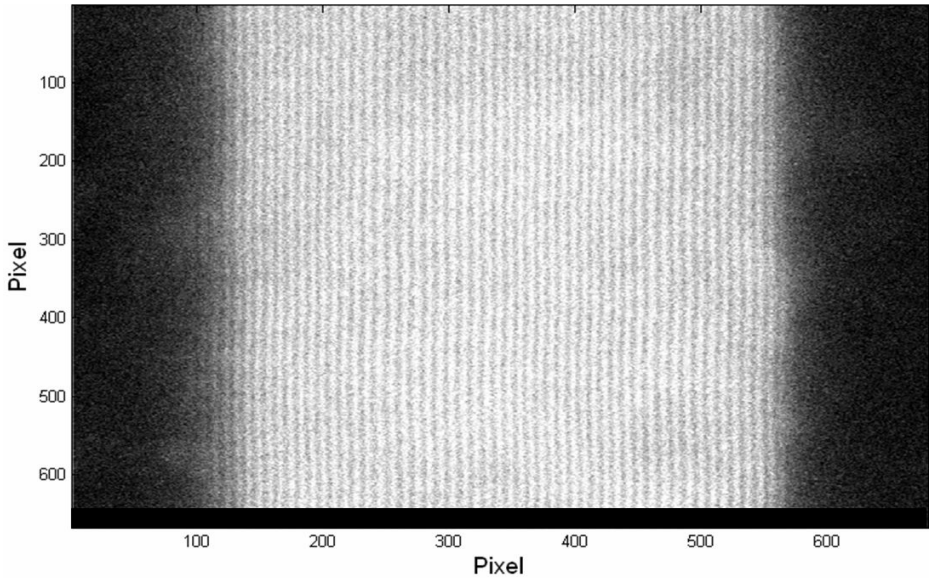

Figure 7: HAADF-STEM image of a SCCDRM feature. The roll-off at the left edge of the image could be due to aberration in the optics.

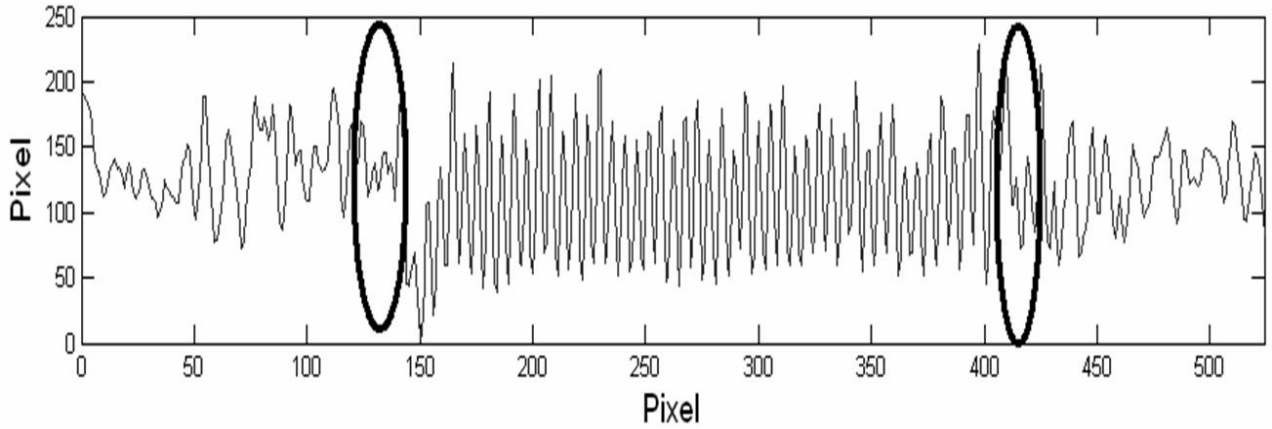

Figure 8: A profile of the center location for the HR-TEM image shown in figure 6. The questionable edge locations are highlighted.

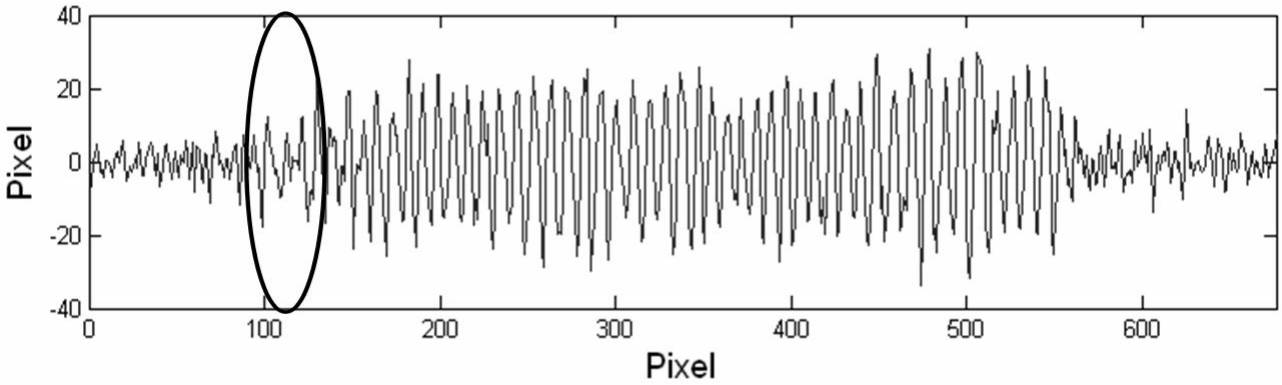

Figure 9: A profile of the center location for the HAADF-STEM image shown in figure 7. The questionable edge locations are highlighted. To enhance signal-to-noise ratio, the above profiles are produced by averaging five scan lines.

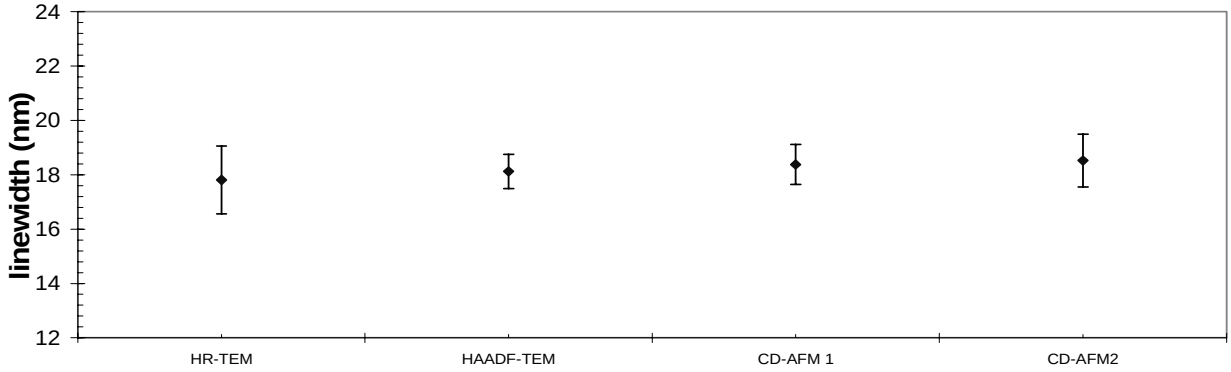

Figure 10: Preliminary results for measurements for HR-TEM, HAADF-STEM, CD-AFM1, and CD-AFM2. Notes: The uncertainties shown are all standard uncertainties $k = 1$. Those for the TEM results include only the uncertainty in edge determination. The uncertainties for the CD-AFM results include all components except for an LWR/navigation term for direct comparison with the TEM values. Note also that the CD-AFM results derive their tip width calibration uncertainty from the independent series of HRTEM samples used in the SCCDRM project.

5. UNCERTAINTY CONSIDERATIONS

One of the main sources of uncertainty in the measurement is the possibility that a different area from where the CD-AFM measurements were taken could be cross-sectioned. This possible source of error could be mitigated by using navigational markers like the one shown in figure 3. Figure 4, which shows portions of the navigational marker, confirms that the sample was indeed cross-sectioned close to the reference line. There is also on-going work to use the linewidth roughness (LWR) of the calibration sample to help relocate the measurement window along the edge [15]. This increases the confidence that the same sample location is being imaged. Figure 11 shows the line width variation data for the CD-AFMs used in this study. The profiles are shifted along the length until they overlap. Based on the overlap of the profiles and the relatively larger LWR in portions of the profile, it is clear that only the shaded location in the profiles could have produced values of ≈18 nm in the TEM measurements.

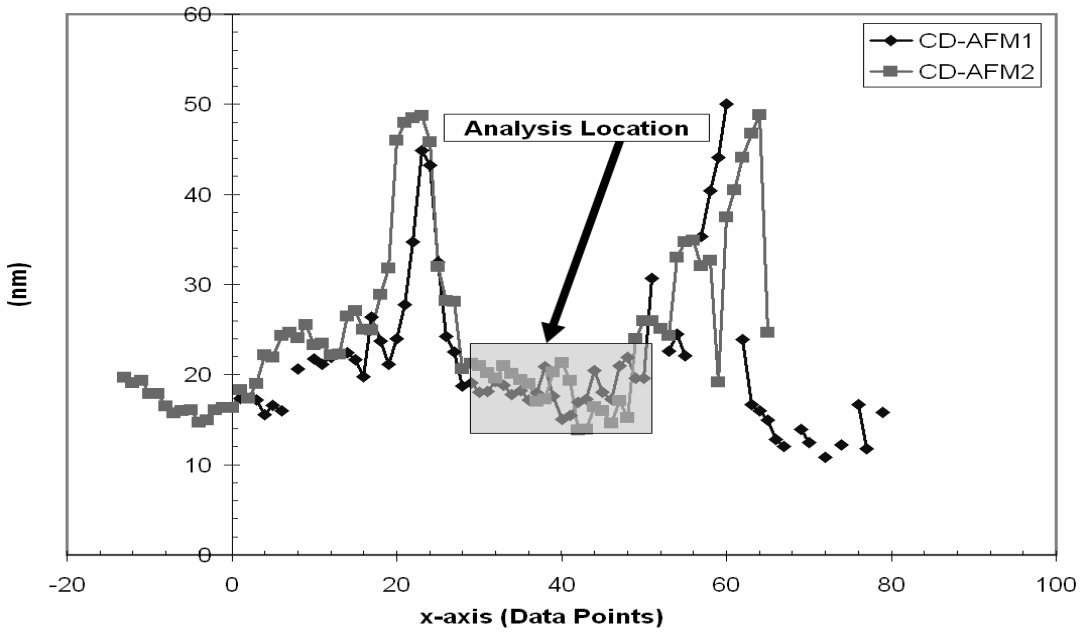

Figure 11: Plots of line width variation from the two CD-AFM. Note that the data for the TEM could have come only from the shaded area for both measurements, which also represents the reference line location for the feature. The data are shifted in the *x*-axis so they can overlap. The missing parts of the profile in the CD-AFM1 profile are due to bad data points.

As indicated, edge location is one of the major sources of error, as shown by the images in figures 5 and 6. In the results presented above, we used the number of lines that could not be attributed to the edge as the preliminary uncertainty. Other potential sources of uncertainty include beam damage to the sample, sample thickness, thickness of the oxide layer, aberrations in the electron optics and sample's orientation related problems. A more thorough analysis that explores such effects and incorporates the resulting uncertainties is being developed.

Additionally, it should be noted that although the physical dimensions of the SCCDRM structures can be well characterized by TEM techniques, these structures are most suitable for CD-AFM tip width calibration. A direct application to scanning electron microscopy (SEM) is not suggested by these results. In the SEM, electron beam and specimen effects are a dominant part of the measurement uncertainty and must be accounted for in order to perform an accurate calibration using any standard.

In recent years, there has been considerable progress in physics-based modeling of the SEM edge bloom by researchers at NIST [16-18]. To perform an accurate SEM calibration, such methods should be used to determine the edge location from the signal, instead of the arbitrary methods (e.g., threshold, max-slope, sigmoidal fit, etc.) that are common in the production environment.

6. CONCLUSION

In this paper, we presented linewidth measurements of an SCCDRM structure using two TEM modes: HR-TEM and HAADF-STEM. Our results show very good agreement – below 0.5 nm – between the two TEM measurements. These results also agreed with measurements of the same structure taken in two different CD-AFMs. The tip widths of these two instruments were independently calibrated using SCCDRM specimens from the 2004 release.

The main source of uncertainty in both TEM measurements was the edge definition. In addition to showing what type of agreement is possible when these two techniques are used, the new HAADF-TEM results offer a separate validation of our earlier HR-TEM calibration for the SCCDRM project. Work on further understanding and accounting for some of the uncertainties of TEM measurements on these structures, such as the oxide thickness and the possible effects of lens aberrations and beam damage to the sample, is currently underway.

ACKNOWLEDGMENTS

NGO is supported by the Office of Microelectronics Programs (OMP) and the Nanomanufacturing Program at NIST. The SCCDRM project is jointly supported by the NIST Advanced Technology Program (ATP) and the OMP. Purchase of supplies for the Dimension X3D™ was supported by several metrology projects at SEMATECH. We thank Alain Diebold of SEMATECH and John Kramar of NIST for valuable comments, and Theodore Vorburger, Michael Postek, Purabi Mazumdar, Jack Martinez, and Steve Knight of NIST for their support and encouragement of this work.

*Address all correspondence to George Orji at George.Orji@nist.gov.

REFERENCES

1. International Technology Roadmap for Semiconductors (ITRS) 2005 Semiconductor Industry Association (SIA) San Jose, CA

2. R. G. Dixson, R. A. Allen, W. F. Guthrie, and M. W. Cresswell, "Traceable Calibration of Critical-Dimension Atomic Force Microscope Linewidth Measurements with Nanometer Uncertainty" *J. Vac. Sci. Technol. B* Vol. **23**, 3028-3032 (2005).

3. A. C. Diebold "Electron Microscopy –Based Measurement of Feature Thickness and Calibration of Reference Materials", in *Handbook of Silicon Semiconductor Metrology*, edited by A. C. Diebold, 851-863, Marcel-Dekker, New York, (2001).

4. B-C Perng, J-H Shieh, S.-M. Jang, M.-S. Liang, R. Huang, L-C Chen, R-L Hwang, J. Hsu and D. Fong "Accurate In-line CD Metrology for Nanometer Semiconductor Manufacturing" *Proc. of SPIE* Vol. **6152** 61520Q-1-9 (2006).

5. C-Y Jeong, J Lee, K-Y Park, W. G. Lee and D-H. Lee "CD-SEM Calibration with TEM to Reduce CD Measurement Error" *Proc. of SPIE* Vol. **4689**, 747-755 (2002).

6. V. A. Ukraintsev, C. Baum, G. Zhang and C. L. Hall "The role of AFM in semiconductor technology development:the 65 nm technology node and beyond" *Proc. of SPIE* Vol. **5752**, 127 -139 (2005).

7. D. B. Williams and C. B. Carter, Transmission Electron Microscopy Plenum, New York, NY (1996).

8. S. J Pennycook, D. E. Jesson, P. D. Nellist, M. F. Chsjolm, N. D. Browning "Scanning Transmission Electron Micorscopy: Z-Contrast" In: Electron Microscopy: Principles and Fundamentals (S. Amelinck, et al., ed.) VCH, Weinheim, (1997).

9. A. C. Diebold, B. Foran, C. Kisielowski, D. A. Muller, S. J. Pennycook, E. Principe, and S. Stemmer "Thin Dielectric Film Thickness Determination by Advanced Transmission Electron Microscopy" *Microsc. Microanal.* **9**, 493–508, (2003).

10. R. Dixson, A. Guerry, M. Bennett, T. Vorburger, B. Bunday, "Implementation of a Reference Measurement System using CD-AFM," *Proc. of SPIE* Vol. **5038**, 150-165 (2003).

11. N. G. Orji, R. G. Dixson, A. Martinez, B. D. Bunday, J. A. Allgair, T. V. Vorburger, "Progress on Implementation of a CD-AFM-Based Reference Measurement System," to be published *in SPIE Journal of Micro/Nanolithography, MEMS and MOEMS*, Vol. **6** (2), (2007).

12. R. Dixson, W. Guthrie, M. Cresswell, R. Allen, N. G. Orji, "Single Crystal Critical Dimension Reference Materials (SCCDRM): Process Optimization for the Next Generation of Standards," to be published in *SPIE Proceedings* Vol. **6518**, (2007).

13. N. G. Orji, R. G. Dixson, "Higher order tip effects in traceable CD-AFM based linewidth measurements," *Meas. Sci. Technol.* **18**, 448-455, (2007).

14. P. J. Mohr and B. N. Taylor, CODATA recommended values of the fundamental physical constants: J. Phys. Chem. Ref. Data **28**(6), 1713-1852 (1999). This paper was also published in Rev. Mod. Phys. **72** (2), 351-495 (2000). The values of these constants are also available online at physics.nist.gov/constants.

15. J. Robert, B. Banke, R. Dixson, "Leveraging LER to Minimize Linewidth Measurement Uncertainty in a Calibration Exercise," to be published in *Proc. of SPIE* Vol. **6518** (2007).

16. J. S. Villarrubia, A. E. Vladar, B. D. Bunday, and M. Bishop, "Dimensional metrology of resist lines using a SEM model-based library approach," *Proc. of SPIE* Vol. **5375**, 199-209 (2004).

17. J. S. Villarrubia, A. E. Vladar, J. R. Lowney, M. T. Postek, "Scanning electron microscope analog of scatterometry," *SPIE Proceedings* Vol. **4689**, 304-312 (2002).

18. J. S. Villarrubia, A. E. Vladar, J. R. Lowney, M. T. Postek, "Edge determination of polycrystalline silicon lines on gate oxide," *SPIE Proceedings* Vol. **4344**, 147 – 156 (2001).